Int. J. Heat Mass Transfer. Vol. 34, No. 1, pp. 103–114, 1991
Printed in Great Britain

0017–9310/91 $3.00 + 0.00

Analysis of the fluid flow and heat transfer in a thin liquid film in the presence and absence of gravity

M. M. RAHMAN, W. L. HANKEY and A. FAGHRI
Department of Mechanical and Materials Engineering, Wright State University, Dayton, OH 45435, U.S.A.

(*Received* 28 *September* 1989 *and in final form* 22 *February* 1990)

Abstract—The hydrodynamic and thermal behavior of a thin liquid film flowing over a solid horizontal surface is analyzed for both plane and radially spreading flows. The situations where the gravitational force is completely absent and where it is significant are analyzed separately and their practical relevance to a micro-gravity environment is discussed. In the presence of gravity, in addition to Reynolds number, the Froude number of the film is found to be an important parameter that determines the supercritical and subcritical flow regimes and any associated hydraulic jump. A closed-form solution is possible under some flow situations, whereas others require numerical integration of ordinary differential equations. The approximate analytical results are found to compare well with the available two-dimensional numerical solutions.

1. INTRODUCTION

MOST EARLIER studies [1–5] on thin film flows are related to the falling film where the motion of the film is driven by the gravitational body force acting in the direction of the flow. These studies covered different areas of application including condensation, evaporation, gas absorption and other chemical processes. With the advancement of technology, however, the thin film flow is also becoming common on horizontal surfaces where the gravitational body force acts perpendicular to the surface or where gravity is entirely absent. In these situations, the film may be generated either by impingement of a jet on a solid wall or by discharge of fluid through a slot from a pressurized container. These situations may occur in the Space Shuttle for inflow to a propellant tank or in the absorber unit of a space-based heat pump absorption system. The understanding of such flows in a micro-gravity environment is essential for the optimal design of fluid flow and heat exchange processes in a space vehicle.

The inviscid flow of a liquid jet impinging on a solid wall is a classical hydrodynamics problem which is available in textbooks [6]. It is concerned with irrotational, incompressible and inviscid flow, in which the effects of gravity and surface tension are neglected. One of the major attractions of this type of approach is that it can be handled using complex potential theory and therefore can be treated analytically.

In nature, however, viscous effects become important, particularly when the thickness of the liquid layer becomes small. Also, gravity cannot be neglected entirely in most situations. Watson [7] analyzed the fluid mechanics of thin films produced by the impingement of a liquid jet on a flat horizontal surface under the action of gravity. By using the boundary layer approximations of the governing transport equations, analytical solutions using a similarity transformation along with the Pohlhausen integral method were derived. The analysis covered the regions where the boundary layer thickness is less than the film height and where the film is totally engulfed by the boundary layer. The possibility of a hydraulic jump in such a flow was also anticipated. However, the analysis was applicable only to the supercritical flow before the jump. The height of the jump was predicted for any given location of the jump. The heat transfer counterpart of the impinging jet problem was considered by Chaudhury [8]. The energy equation was solved in closed form including the effects of viscous dissipation by approximating the temperature profile with a fourth-order polynomial. Nusselt numbers for different Prandtl numbers were presented.

The impingement of a liquid jet in a gravity-free environment was presented by Labus and DeWitt [9]. They included the effects of surface tension, but entirely neglected the viscous forces. From a scaling analysis, it was shown that for a large jet Reynolds number, the flow can be approximated to be inviscid. Numerical solutions of the governing transport equations were obtained and compared with experimental measurements. Three distinct flow patterns of the jet were obtained which were classified in accordance with relative importance of inertia and surface tension.

In the studies mentioned above, the investigators considered either inviscid flow or viscous supercritical flow up to the location of the jump. The fluid flow in the vicinity of the jump or in the subcritical region following the jump is also important from an engineering point of view. In fact, under a moderate gravi-

NOMENCLATURE

A	flow parameter, defined by equation (14)
c_f	friction coefficient, $\tau_w/(0.5\rho W^2)$
Fr	Froude number, $W/\sqrt{(g\delta)}$
g	acceleration due to gravity [m s^{-2}]
h	heat transfer coefficient [W m^{-2} K^{-1}]
k	thermal conductivity [W m^{-1} K^{-1}]
K	coordinate parameter: 0, for plane flow; 1, for radial flow
L	length of the plate [m]
Nu^*	Nusselt number in terms of film height, $h\delta/k$
p	static pressure [Pa]
q	heat flux [W m^{-2}]
Q	volumetric flow rate (per unit width for plane flow) [m^3 s^{-1}]
r	radial coordinate
R	dimensionless radius, defined by equations (45) and (50)
$R1$	dimensionless radius, defined by equations (22) and (26)
Re	Reynolds number, $W\delta/\nu$
t	time [s]
T	temperature [K]
v	component of velocity normal to the plate [m s^{-1}]
$\mathbf{V}$	velocity vector [m s^{-1}]
w	component of velocity along the plate [m s^{-1}]
W	average velocity along the plate [m s^{-1}]
y	coordinate normal to the plate
z	coordinate along the plate.

Greek symbols

α	thermal diffusivity [m^2 s^{-1}]
β	flow parameter (defined by equation (54))
δ	film thickness [m]
δ_B	thickness of momentum boundary layer [m]
η	dimensionless coordinate normal to the plate, y/δ
μ	dynamic viscosity [N s m^{-2}]
ν	kinematic viscosity [m^2 s^{-1}]
ρ	density [kg m^{-3}]
τ	shear stress [N m^{-2}].

Subscripts

b	mixed mean (bulk) condition
e	condition on the free surface
in	condition at entrance
out	condition at exit
sat	saturation condition
w	condition on solid wall.

Superscript

*	critical condition in the flow.

tational field, a jump will always be present in a horizontal rotating absorber unit during start-up and operation at small rates of rotation and small flow rates. Moreover, all of the studies mentioned above are concerned with a thin film formed by impingement of a liquid jet. The driving mechanism of these flows are flow rate and jet diameter which are characterized by jet Reynolds number. So, the findings in these studies cannot be applied readily to a situation where the film is formed by discharge from a pressurized container. This situation was considered in recent studies [10–12]. A systematic numerical study of two-dimensional fluid flow and heat transfer in a thin liquid film in both plane and radially spreading flows was performed. The studies covered both zero and normal gravity environments. In the absence of gravity, no jump was found and the flow remained supercritical in the entire domain. In the presence of gravity, a jump was found under some flow conditions. In all of these studies, the flow field was computed numerically using a boundary-fitted coordinate system where the irregular free surface of the film was taken as one of the boundaries of the computation domain. The inertial, viscous and pressure forces were identified to be dominant and the surface tension was found to be negligible in most regions.

The computational methodology presented in refs. [10, 12] is termed the 'pressure optimization method' where the shape of the free surface was represented by an algebraic equation with two or more arbitrary constants. The constants were optimized using an exhaustive search which minimized the difference between the computed free surface and ambient pressures. The method was found to be robust and was extremely satisfactory for zero-gravity flows. However, when a jump was present in the computation domain, the pressure optimization method was unable to compute the jump as a single-domain problem. The subcritical and supercritical flows were computed separately and were matched at the jump interface preserving the conservation of mass, momentum and energy.

The two-dimensional numerical method presented in ref. [11] is termed 'porous wall method'. In this method, the free surface was assumed to be a permeable wall where fluid particles could cross this boundary depending on the difference between the fluid and ambient pressures. The shape of the surface was improved by successive iterations until the free surface conformed to a streamline where no penetration occurred. This method proved to be successful in handling the regions before and after the

jump as a single-domain problem. The details of the flow structure in the vicinity of the jump were presented along with values of the skin friction and heat transfer coefficients.

Even though the complete numerical solution for the flow field and heat transfer coefficient [10–12] are available, the need for a simple, systematic, analytical method to describe the flow is inevitable. The numerical results are limited to the flow parameters used for the computation, and cannot be extended in general. Moreover, an analytical expression is easier to use and implement in addition to the understanding of the limiting behavior of the flow. The present work is intended to analyze both zero-gravity flows and the flows where gravity is significant. The application of these results in a micro-gravity situation will be examined. Unlike previous analytical studies, it will cover both supercritical and subcritical regions and the jump connecting the two domains. In addition to analyzing the flow field, the heat transfer will be studied.

2. EQUATIONS OF MOTION

The schematic of the problem under consideration is shown in Fig. 1. A thin liquid film is flowing adjacent to a solid heated wall. Two classes of flows are considered here.

(a) Plane flow: where the film moves in a two-dimensional fashion along a plane horizontal wall.

(b) Axisymmetric radial flow: where the liquid is introduced at the center of a circular horizontal plate and spreads out radially.

The $z(r)$-axis is directed along the longitudinal (radial) direction, and the y-axis is directed normal to the plate. The velocity components in these two directions are w and v, respectively. The height of the free surface from the solid wall is denoted by δ which varies with the longitudinal (radial) location of the plate.

The equations governing the conservation of mass, momentum and energy for an incompressible constant-property flow are given by

$$\nabla \cdot \mathbf{V} = 0 \tag{1}$$

$$\frac{\mathrm{D}\mathbf{V}}{\mathrm{D}t} = -\frac{1}{\rho}\nabla p + \nu\nabla^2\mathbf{V} + \mathbf{g} \tag{2}$$

$$\frac{\mathrm{D}T}{\mathrm{D}t} = \alpha\nabla^2 T. \tag{3}$$

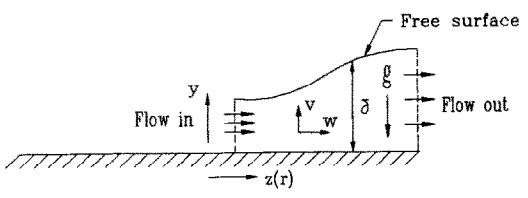

FIG. 1. Schematic of the physical problem.

Here we have also assumed that heat generation due to viscous dissipation and pressure work are negligible. The velocity vector $\mathbf{V}$ can be resolved into components as

$$\mathbf{V} = w\mathbf{k} + v\mathbf{j}.$$

The vectorial representation used in equations (1)–(3) is easier to handle since it can be readily transformed to Cartesian or cylindrical components as needed. The boundary conditions in component form are given by

at $y = 0$:

$$v = w = 0$$

$$\begin{cases} T = T_w, & \text{for isothermal wall} \\ -k\dfrac{\partial T}{\partial y} = q_w, & \text{for constant flux wall} \end{cases} \tag{4}$$

at $y = \delta$:

$$\frac{\mathrm{d}\delta}{\mathrm{d}z} = \frac{v}{w}, \quad p = p_e, \quad \frac{\partial w}{\partial y} = 0$$

$$\begin{cases} T = T_{sat}, & \text{for evaporation} \\ \dfrac{\partial T}{\partial y} = 0, & \text{for adiabatic condition} \end{cases} \tag{5}$$

at $z = 0$ or $r = r_{in}$:

$$w = W_{in}, \quad T = T_{in} \tag{6}$$

at $z = L$ or $r = r_{out}$:

$$\frac{\partial p}{\partial y} = -\rho g, \quad \frac{\partial T}{\partial z} = 0$$

$$\begin{cases} \dfrac{\partial w}{\partial z} = 0, & \text{for zero gravity} \\ Fr = Fr_{out}, & \text{for non-zero gravity.} \end{cases} \tag{7}$$

On the free surface, both streamline and stress-free conditions have to be satisfied. The balance of normal stresses, in general, relate fluid pressure to the ambient pressure via surface tension and other stresses. From a scaling analysis, it can be shown that [11], for a reasonably large Weber number and flow rate that is typical for these flows, these stress terms are found to be an order of magnitude lower than the pressure. So, the surface tension can be assumed to be negligible in most regions of the flow leading to the $p = p_e$ condition on the free surface.

Both plane and radial flows described above will be solved for zero and normal gravity situations. In the following two sections, we will analyze the flow using uniform and parabolic velocity distributions, respectively. The former is more common in fluid flow literature concerning a hydraulic jump or shock wave and will be carried out in detail. The latter section will improve on the analysis by using a parabolic velocity distribution across the film, which is more appropriate for laminar thin film flow.

3. ANALYSIS OF FLOW USING ONE-DIMENSIONAL UNIFORM VELOCITY

We first consider the situation where the velocity variation across the thickness of the film is neglected, and the film is assumed to propagate downstream with its uniform average velocity. Let W be the average velocity of the film in the longitudinal (radial) direction of the plate and Q be the volumetric flow rate. In the case of plane flow, Q is the volume flow rate per unit width. The continuity equation (1) can be written as

$$Q = (2\pi r)^K \delta W \tag{8}$$

where

$$K = \begin{cases} 0, & \text{for plane system} \\ 1, & \text{for radial system.} \end{cases}$$

Integrating equation (2) across the thickness of the film, expressing the resistance from the solid wall in terms of friction coefficient and substituting equation (8) results in

$$\frac{\mathrm{d}}{\mathrm{d}r}\left(\frac{W^2}{2} + g\delta\right) = -\frac{c_f}{2}\frac{W^2}{\delta}. \tag{9}$$

This momentum equation must be solved along with equation (8) to determine the flow field, and will be carried out in the following subsections.

3.1. *Flow under zero gravity*

For a steady flow under zero gravity, the governing equations (8) and (9) reduce to

$$Q = (2\pi r)^K \delta W = \text{constant} \tag{10}$$

$$W\frac{\mathrm{d}W}{\mathrm{d}r} = -\frac{c_f}{2}\frac{W^2}{\delta}. \tag{11}$$

Eliminating δ from equations (10) and (11) gives

$$W^{-2}\,\mathrm{d}W = -\frac{c_f}{2Q}(2\pi r)^K\,\mathrm{d}r.$$

Integrating this equation assuming a constant c_f and substituting the conditions at one location of the flow (i.e. at $r = r_{in}$, $W = W_{in}$ and $\delta = \delta_{in}$) yields the solution in the form

$$\frac{W}{W_{in}} = \frac{1 - \frac{c_f}{2}\frac{r}{(K+1)\delta}}{1 - \frac{c_f}{2}\frac{r_{in}}{(K+1)\delta_{in}}} = \frac{\delta_{in}}{\delta}\left(\frac{r_{in}}{r}\right)^K. \tag{12}$$

Solving for δ results in the following relation:

$$\frac{\delta}{\delta_{in}} = A\frac{r}{r_{in}} + (1-A)\left(\frac{r_{in}}{r}\right)^K \tag{13}$$

where

$$A = \frac{c_f}{2}\frac{r_{in}}{(K+1)\delta_{in}}. \tag{14}$$

From equation (13) we may express the distribution of film height for plane and radial flows. For plane flow ($K = 0$), the equation simplifies to

$$\frac{\delta}{\delta_{in}} = 1 + \frac{c_f}{2}\frac{z}{\delta_{in}}. \tag{15}$$

This indicates that for a constant friction coefficient the film height increases linearly with distance. This increase in film height is because of the decrease in flow velocity due to the resistance from the wall. We may also notice that for inviscid flow when no resistance is exerted by the solid wall, the film height remains the same at all downstream locations beginning from the entrance.

In real flow situations, however, the friction coefficient varies along the plate. Usually, near the entrance the friction coefficient is greater due to the rapid changes in the velocity profile as the boundary layer develops beginning from the entrance plane. A good estimate of the friction coefficient can be made using the Blasius solution [13] for forced convective boundary layer adjacent to a plate. This results in

$$c_f = \frac{0.664}{\sqrt{\left(\frac{Wz}{\nu}\right)}}, \text{ for plane flow} \tag{16a}$$

and

$$c_f = \frac{0.664}{\sqrt{\left(\frac{W(r-r_{in})}{\nu}\right)}}, \text{ for radial flow.} \tag{16b}$$

However, unlike any other external flow, in a thin film the boundary layer thickness is frequently of the order of the film height. So, after some distance downstream, the viscous effects propagate all the way to the free surface. Then c_f can be better estimated from the equation presented in a later section of this paper (equation (46)). The location where one should switch over from one formulation to the other may be estimated from the solution of the boundary layer thickness for forced convection. The thickness of the momentum boundary layer is given by

$$\delta_B = 5.0\sqrt{\left(\frac{\nu z}{W}\right)}, \text{ for plane flow}$$

and

$$\delta_B = 5.0\sqrt{\left(\frac{\nu(r-r_{in})}{W}\right)}, \text{ for radial flow.}$$

As shown by Thomas *et al.* [14], the two friction factor estimates yield the same value at $\delta = 1.81\delta_B$. So, for continuity, one may use equation (16) for $\delta/\delta_B > 1.81$ and equation (46) for $\delta/\delta_B < 1.81$.

The one-dimensional analytical solution with the friction coefficient described above has been compared with the numerical solution of ref. [10] in Fig. 2 for $Re = 12.5$, $L = 0.03$ m, $\delta_{in} = 0.000595$ m and

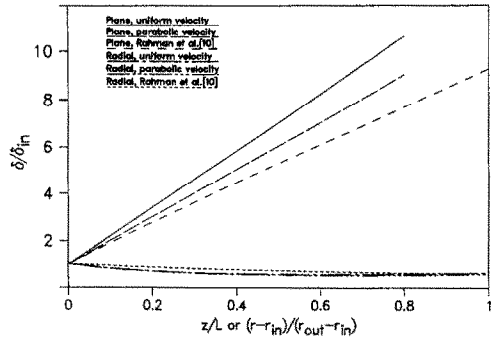

FIG. 2. Film height for plane and radial flows under zero gravity.

$\nu = 7.4 \times 10^{-6}$ m^2 s^{-1} for plane flow. Similar to the analytical solution, a uniform inlet velocity has been assumed for the numerical solution. The predicted film height distribution is found to be somewhat higher than the two-dimensional numerical solution. A test run with the friction coefficient reported in ref. [10] yielded a solution almost coincident with the numerical film height. So, the discrepancy is primarily due to approximations inherent with the estimation of the friction coefficient. The Blasius solution is perfectly valid for boundary layer flow where the free stream extends through a large distance and no free surface is present. However, the comparison is reasonable considering the approximations inherent in the simple analytical formulation.

A plot of equation (13) for radial flow under zero gravity is presented in Fig. 3 for different values of A. For $A = 0.0$, which corresponds to inviscid flow, the film height monotonically decreases with radial distance. This is quite expected since, in the absence of any friction, the velocity of fluid particles will remain constant. Therefore, the film height has to decrease with radius as more and more area becomes available to the flow. In this plot we also notice that when friction is present ($A > 0$), the film height may increase or decrease depending on the value of A and the radial location. Also, for a given radial location the value of the film height is more for a larger value of A, since A quantifies the frictional resistance compared to the inertial forces. For $A = 0.2$ and 0.4, the film height decreases first, attains a minimum and then increases further downstream. The location for minimum δ can be determined by differentiating equation (13) which gives

$$\left(\frac{r}{r_{in}}\right)_{\text{for min }\delta} = \left(\frac{1-A}{A}\right)^{1/2} \tag{17}$$

$$\left(\frac{\delta}{\delta_{in}}\right)_{min} = 2\sqrt{A}\sqrt{(1-A)}. \tag{18}$$

From equation (17) we find that a minimum exists if $A < 1/2$. Otherwise, the film height increases continuously from the entrance as seen in plots corresponding to $A > 0.5$. At $A = 1.0$, the film height increases linearly with radius.

The analytical solution for a particular case of $Re_{in} = 404$, $\delta_{in} = 0.005$ m, $r_{in} = 0.05$ m, $r_{out} = 0.2$ m and $\nu = 7.4 \times 10^{-6}$ m^2 s^{-1} is shown in Fig. 2 where it is compared to the two-dimensional numerical solution given in ref. [10]. Here, we have also used the friction coefficient estimated by equations (16) and (46). The results are very close except for the fact that the analytical solution shows a minimum in the flow domain. The minimum is indeed present as verified from the value of A. The numerical solution could not accommodate this behavior since a continuous hyperbolic curve was assumed to represent the free surface.

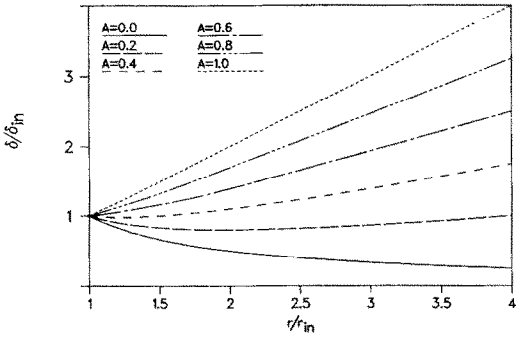

FIG. 3. Analytical film height for radial flow under zero gravity.

3.2. *Flow in the presence of gravity*

When the gravitational body force is significant compared to other existing forces, its effect should be included in the analysis. Unlike a regular forced or natural convection flow in outer space, the effect of gravity, even small, may be significant in a thin film flow since two potential flow regimes, namely supercritical and subcritical may be encountered. These regimes are characterized by the Froude number. The transition of the flow from supercritical to subcritical is analogous to the transition from supersonic to subsonic flow in gas dynamics, where the Mach number determines which regime is present. The analysis presented below uses the methodology commonly followed in the analysis of high speed flow with friction (i.e. Fanno flow). The application of these ideas to a thin film flow is entirely new and it enabled us to combine both flow regimes (supercritical and subcritical) in a single analysis which was not possible by previous investigators. Most previous analytical studies assumed the film height to remain constant in the subcritical region. Expressing equations (8) and (9) in terms of the Froude number results in

$$Q = (2\pi r)^K \sqrt{g}\, Fr\, \delta^{3/2} \tag{19}$$

$$\frac{d}{dr}\left[\delta\left(1+\frac{Fr^2}{2}\right)\right] = -\frac{c_f}{2} Fr^2. \tag{20}$$

These equations will be solved for plane and radial flows in the following subsections.

3.2.1. *Plane flow.* For plane flow $K = 0$, so equations (19) and (20) can be combined by eliminating the film height and nondimensionalized assuming c_f to be locally uniform to give the equation

$$(1-Fr^2)\frac{dFr}{dR1} = \frac{9}{2}Fr^{11/3} \tag{21}$$

where

$$R1 = \frac{z}{\frac{6}{c_f}(v^2/g)^{1/3}\,Re^{2/3}}. \tag{22}$$

Integration of equation (21) gives

$$\frac{1}{12}Fr^{-8/3} - \frac{1}{3}Fr^{-2/3} = -R1 + c.$$

To evaluate the integration constant, the Froude number must be specified at one location in the flow. Upon examining equation (21) we notice that the equation is singular at $Fr = 1$, so a critical flow situation is present at that location. This is analogous to a Mach number of unity in a compressible flow. Let this critical location be denoted by $R1^*$. Then the solution can be written as

$$R1 - R1^* = -\frac{1}{4} + \frac{1}{3}Fr^{-2/3} - \frac{1}{12}Fr^{-8/3}. \tag{23}$$

Equation (23) is a double-valued function as shown (in circles) in Fig. 4. The two branches of the function represent subcritical or supercritical flows where the Froude number is less than or greater than unity, respectively.

Since two solutions exist at any location, the possibility of a sudden jump from supercritical to subcritical flow exists. The opposite is not true since that would violate the second law of thermodynamics. The height of the film before and after the jump can be related by the conservation of mass and momentum across the jump. This is given by

$$\frac{\delta_2}{\delta_1} = \frac{1}{2}[\sqrt{(1+8Fr_1^2)} - 1] \tag{24}$$

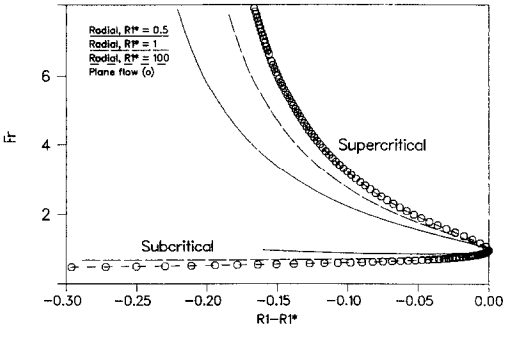

FIG. 4. Analytical solution for plane and radial flows over a plate in the presence of gravity (uniform velocity).

where subscript 1 indicates conditions before the jump and subscript 2 indicates conditions after the jump.

In Fig. 4, it can be observed that both subcritical and supercritical flows move towards the critical condition. In the supercritical regime, the Froude number decreases downstream, whereas in the subcritical regime it increases with distance. Since the Froude number is inversely related to the film height, the film height is expected to increase downstream in the supercritical region and decrease downstream in the subcritical region. A flow starting with $Fr < 1$ will follow the subcritical curve all the way to the exit. However, a flow starting with $Fr > 1$ may follow the supercritical curve all the way to the exit or may encounter a jump and transform to subcritical flow inside the region under consideration. The location of the jump is determined by the downstream condition of the flow.

3.2.2. *Axisymmetric radial flow.* For radial flow, $K = 1$, equations (16) and (17) may be transformed into the following form:

$$(1-Fr^2)\frac{dFr}{dR1} = \frac{9}{2}Fr^{11/3} - \frac{Fr(2+Fr^2)}{2R1} \tag{25}$$

where

$$R1 = \frac{r}{\frac{6}{c_f}(v^2/g)^{1/3}\,Re^{2/3}}. \tag{26}$$

Analogous to plane flow, here the radial distance has been nondimensionalized using the local Reynolds number and friction coefficient. The variation of friction coefficient with radial distance has been assumed to be negligible. A closed-form solution of equation (25) is not possible, so a numerical integration was performed using the Euler method. It can be noticed that the equation is singular at $Fr = 1$. Therefore, the critical condition cannot be directly applied as a boundary condition in the numerical solution. To avoid this singularity, the equation can be expanded around the singular point and the solution can be found at a short distance from the singular point from the lowest-order expansion. The numerical integration then can be carried out beginning from a short distance away from the singular point, where the solution is already known. The solution is shown in Fig. 4.

It should be noted that the critical radius, $R1^*$, appears as a parameter. For a given flow rate and inlet Froude number, the value of $R1^*$ depends on the inlet radius. A large $R1^*$ indicates that the flow starts up at a larger radial distance, where the effect of curvature is smaller. This is quite evident from the plot since the result for $R1^* = 100$ coincides with the solution for the plane flow. The double-valued nature of the solution is also present in radial flow which also indicates the possibility of a hydraulic jump. The film height before and after the radial jump can be related by the same equation as for plane flow (equation (24)).

3.3. *Characteristic behavior of the flow*

Since the equations of transport for the free surface flow of a thin liquid film are somewhat similar to those for one-dimensional compressible flow, it may be useful to analyze the characteristic behavior of the flow.

The conservation equations in the time-dependent form can be written as

$$\frac{\partial U}{\partial t}+\frac{1}{r^K}\frac{\partial}{\partial r}(r^K E)=H$$

where

$$U=\begin{vmatrix}\delta\\ \delta W\end{vmatrix},\quad E=\begin{vmatrix}\delta W\\ \delta\left(W^2+\dfrac{g\delta}{2}\right)\end{vmatrix}$$

and

$$H=\begin{vmatrix}0\\ -\tau_w/\rho\end{vmatrix}$$

where τ_w is the surface shear stress. These are two first-order partial differential equations in t and r with two dependent variables, δ and W.

These two equations may be linearized and written in the following characteristic form:

$$R_t+CR_x=S$$

where

$$R=\begin{vmatrix}W+\sqrt{(g\delta_1)}\dfrac{\delta}{\delta_1}\\ W-\sqrt{(g\delta_1)}\dfrac{\delta}{\delta_1}\end{vmatrix}=\text{Riemann invariants}$$

$$C=\begin{vmatrix}W_1+\sqrt{(g\delta_1)}\\ W_1-\sqrt{(g\delta_1)}\end{vmatrix}=\text{wave speed.}$$

It can be seen that the first invariant always propagates downstream (i.e. $C>0$). The second invariant, however, propagates downstream for supercritical flow ($Fr=W_1\sqrt{(g\delta_1)}>1$) and propagates upstream for subcritical flow ($Fr<1$). This implies that both W and δ must be prescribed upstream for solving supercritical flows while only one is prescribed upstream and one downstream for solving subcritical flows.

3.4. *Application of results to micro-gravity*

The zero-gravity thin film flow considered here can be attained only in a complete absence of the gravitational body force. However, in orbit the gravity is very small, but not precisely zero. Therefore, the range of applicability of the results needs to be investigated. Looking at plane flow results under zero gravity we notice that

$$\delta=\left(\frac{c_f}{2}\right)z+\delta_{in}.$$

This suggests a monotonic increase in the film height so long as c_f remains positive. The flow decelerates due to friction and consequently the film height increases. Since the major driving mechanism for this flow is inertia, a film introduced with a finite velocity becomes very slow after traveling a certain distance.

When investigating the expression for the Froude number, it can be noticed that even for a very small gravity force, where the inlet Froude number tends to infinity, the Froude number may become of the order of unity after some distance, since both the deceleration of flow and the increase of film height contribute to reducing the Froude number. The situation here is analogous to hypersonic flow, which in the presence of friction rapidly ceases to be hypersonic after traveling some distance. Therefore, in a microgravity situation, the order of magnitude of the local Froude number is very important. When the Froude number is extremely large, like near the entrance, the zero gravity results may be applicable. However, away from the entrance, when the velocity (W) becomes small and consequently Froude number ($W/\sqrt{(g\delta)}$) becomes finite, one may resort to the normal gravity results presented here.

4. ANALYSIS OF FLOW AND HEAT TRANSFER USING PARABOLIC VELOCITY DISTRIBUTION

The one-dimensional analysis presented in the previous section revealed many interesting features of the flow. However, the velocity profile in reality is two-dimensional in nature because of the no-slip condition at the solid wall. As demonstrated in ref. [10], the velocity profile is approximately parabolic in nature in most regions of the flow. The temperature profile may also become parabolic after the thermal boundary layer develops.

We assume the velocity component, w, and temperature, T, to have the following general form where the boundary condition at the solid wall and free surface are satisfied:

$$\frac{w}{W}=3\eta\left(1-\frac{\eta}{2}\right) \tag{27}$$

$$\frac{T}{T_w}=1+B\eta+C\eta^2 \tag{28}$$

where η is the dimensionless coordinate across the thickness of the film. The constants B and C will be evaluated later in this section for different thermal conditions considered here.

Once the velocity and temperature profiles are fixed, the other flow quantities can be readily calculated and are given as follows:

$$\tau_w=\frac{3\mu W}{\delta} \tag{29}$$

$$q_w=-\frac{kBT_w}{\delta} \tag{30}$$

$$q_e = -\frac{kT_w}{\delta}(B+2C) \tag{31}$$

$$T_e = T_w(1+B+C) \tag{32}$$

$$T_b = T_w\left(1+\frac{5}{8}B+\frac{9}{20}C\right). \tag{33}$$

In a thin film flow, the velocity across the thickness of the film is much smaller than the velocity along the plate. Scaling governing equations (1)–(3) using the condition $v \ll w$ gives

$$\frac{1}{r^K}\frac{\partial}{\partial r}(r^K w)+\frac{\partial v}{\partial y}=0 \tag{34}$$

$$w\frac{\partial w}{\partial r}+v\frac{\partial w}{\partial y}=-\frac{1}{\rho}\frac{\partial p}{\partial r}+\nu\frac{\partial^2 w}{\partial y^2} \tag{35}$$

$$-\frac{1}{\rho}\frac{\partial p}{\partial y}+g=0 \tag{36}$$

$$w\frac{\partial T}{\partial r}+v\frac{\partial T}{\partial y}=\alpha\frac{\partial^2 T}{\partial y^2}. \tag{37}$$

Here $K=0$ indicates plane flow and $K=1$ denotes radial flow. Integrating equation (36) we get

$$p = p_e+\rho g(\delta-y) \tag{38}$$

where p_e is the pressure at the edge of the free surface. This indicates that the pressure across the thickness of the film is hydrostatic in nature. Also, at zero gravity, $p=p_e$. In the external flow over a flat surface, the ambient pressure usually remains constant. So, in a gravity-free environment, the static pressure is expected to remain constant everywhere in the flow field.

4.1. *Plane flow under zero gravity*

For plane flow under zero gravity equations (34) and (35) can be integrated from 0 to δ using the velocity profile given in equation (27) and the no-slip condition at the solid wall and zero-shear condition at the free surface. After using the definition of Reynolds number, it results in the relationship

$$\frac{d\delta}{dz}=\frac{2.5}{Re}. \tag{39}$$

Integrating this equation, one obtains

$$\frac{\delta}{\delta_{in}}=1+\frac{2.5}{Re}\frac{z}{\delta_{in}}. \tag{40}$$

For plane flow, the Reynolds number remains constant. Therefore, the film height increases linearly beginning from the entrance location. We also notice that in the limiting case of $Re\to\infty$, $\delta=\delta_{in}$ everywhere in the flow field. This is quite expected since in an inviscid plane flow, the film height remains constant.

Figure 2 shows a comparison of this solution with previous numerical results of ref. [10]. The analytical solution tends to predict a somewhat higher film height than the numerical solution, but lower than the solution predicted by assuming a uniform one-dimensional velocity distribution. The assumption of a parabolic velocity profile, even though not exact everywhere in the flow field, produces a reasonable estimate of the film height distribution.

4.2. *Radial flow under zero gravity*

For radial flow under zero gravity, the integrated equation for the conservation of momentum can be written as

$$\frac{d\delta}{dr}=\frac{2.5}{Re}-\frac{\delta}{r}. \tag{41}$$

Analogous to the plane flow case, we have used the continuity equation, the boundary conditions at the solid wall and free surface and the definition of Reynolds number to arrive at this relationship. Note that this equation reduces to the plane flow equation as $r\to\infty$. We can also observe that $d\delta/dr$ can be positive or negative. So, the film height may increase or decrease in the case of radial flow, in contrast to plane flow, where a linear increase is encountered. The frictional resistance at the solid wall reduces the flow velocity and consequently tends to increase the height. However, at the same time, the flow is spreading radially with more area available for the flow as the radius increases. This same behavior was seen in the discussion of one-dimensional analysis (Fig. 3), where the parameter 'A' determined the variation of film height downstream from the entrance. 'A' is a function of inlet Reynolds number along with inlet height and radius. Note also that the Reynolds number does not remain constant in radial flows and changes with location.

Integrating equation (41) gives

$$\frac{\delta}{\delta_{in}}=\frac{r_{in}}{r}+\frac{2.5(r^3-r_{in}^3)}{3Re_{in}\,r\delta_{in}r_{in}}. \tag{42}$$

The location of the minimum film height may be calculated by differentiating equation (42) with respect to r. This results in

$$(r)_{\text{for min }\delta}=r_{in}\left[\frac{3Re_{in}\,\delta_{in}}{5}\left(\frac{1}{r_{in}}-\frac{5}{6Re_{in}\,\delta_{in}}\right)\right]^{1/3}. \tag{43}$$

We can also notice that the minimum will exist when

$$\frac{Re_{in}\,\delta_{in}}{r_{in}}\leq\frac{5}{2}.$$

The results of the analytical solution for radial flow under zero gravity is also compared with previous numerical results of ref. [10] in Fig. 2. In this case, we can see a minimum inside the flow domain confirming the observation from the one-dimensional analytical solution using the uniform velocity profile. Both analytical solutions are close to each other whereas the numerical solution is slightly higher in most parts of the flow.

4.3. *Plane flow in the presence of gravity*

For plane flow where the gravitational body force term in retained, the governing equations of motion, equations (34) and (35), can be integrated across the thickness of the film using equation (38), the boundary conditions, and the definition of Reynolds number, and can be transformed to the equation

$$\left(\frac{5}{6}-Fr^2\right)\frac{dFr}{dR}=\frac{15}{4}Fr^{11/3} \tag{44}$$

where

$$R=\frac{z}{(\nu^2/g)^{1/3}\,Re^{5/3}}. \tag{45}$$

Here the radial coordinate R is normalized in terms of Reynolds number. Note that the definition of R is very similar to the normalized radius Rl used in the one-dimensional analysis using the uniform velocity except that the friction coefficient c_f appears in Rl whereas it does not appear in R. From equation (29), the friction coefficient can be easily calculated to be

$$c_f=\frac{6}{Re}. \tag{46}$$

This friction coefficient is correct when the velocity profile is parabolic across the thickness of the film, which obviously assumes that viscous effects are extended all the way to the free surface. When this definition of c_f is assumed, Rl becomes the same as R. In the present investigation we have tried to keep the one-dimensional analysis using the uniform velocity somewhat more general where any known distribution of the friction coefficient may be used.

From equation (44) it can be noticed that a critical condition in the flow occurs at $Fr = 0.913$. Note that this value of Froude number is different from the conventional critical Froude number of $Fr = 1$, which is strictly valid for a one-dimensional flat velocity distribution. The Froude number of 0.913 is therefore the 'weighted' value for the parabolic profile. Integrating equation (44) with a boundary condition of $R = R^*$ at $Fr = 0.913$ we can obtain the solution as

$$-1.195+\frac{3}{2}Fr^{-2/3}-\frac{5}{16}Fr^{-8/3}=3.75(R-R^*). \tag{47}$$

A plot of this equation is shown in Fig. 5 (as circles). Analogous to the one-dimensional analysis, the solution is also found here to be double valued in nature. The two stems of the curve denote the supercritical and subcritical flow regimes. The possibility of a hydraulic jump also exists here, which basically depends on the incoming Froude number, length of the plate and flow condition at the outlet. The jump may be present only when the flow initially is supercritical. The ratio of the film height before and after the jump can be determined from a mass and momentum balance at the jump, which, in this case, turns out to be

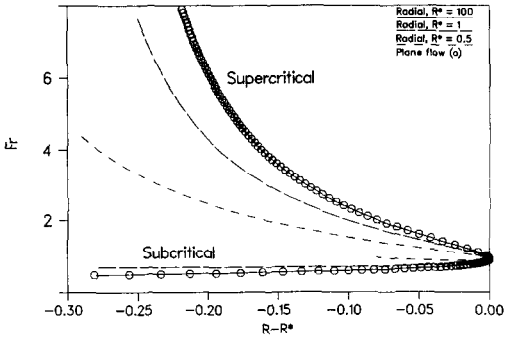

FIG. 5. Analytical solution for horizontal flow over a plate in the presence of gravity (parabolic velocity).

$$\frac{\delta_2}{\delta_1}=\frac{1}{2}[\sqrt{(1+9.6Fr_1^2)}-1] \tag{48}$$

where subscript 1 indicates conditions before the jump and subscript 2 indicates conditions after the jump. In comparing this relationship with equation (24) for uniform flow only the coefficient within the radical changes for the parabolic profile.

Plane flow in the presence of gravity is characterized by two independent dimensionless groups, namely, the Froude number and Reynolds number. Since the Reynolds number is lumped with other parameters in the definition of R, to see its effects more clearly, the plane flow solution is plotted again in Fig. 6 for different values of Reynolds number using $(z-z^*)/(\nu^2/g)^{1/3}$ as the abscissa. Note that for a small Reynolds number, the supercritical solution cannot be sustained for a large length of the plate. On the other hand, for the same Reynolds number, the subcritical solution may be present for any length of the plate. Also, the length for which a supercritical solution may be present increases with Reynolds number. So, for a given length of the plate and inlet Froude number, the length of the supercritical flow regime is directly dependent on the Reynolds number. For a

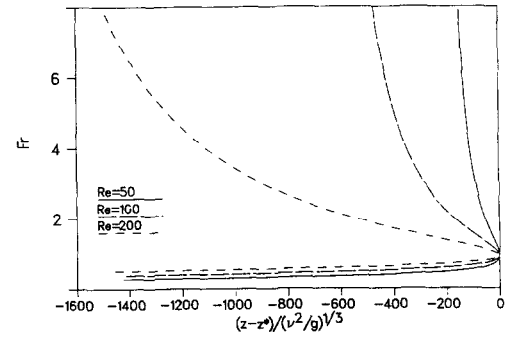

FIG. 6. Froude number distribution for plane flow over a plate in the presence of gravity.

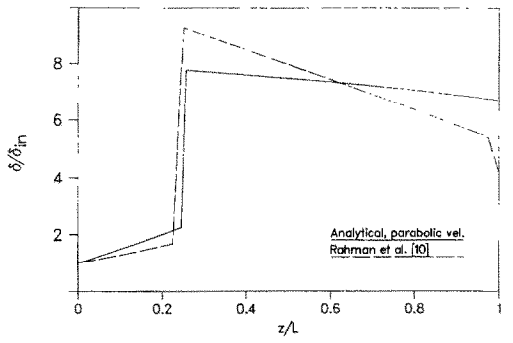

FIG. 7. Comparison of predicted film height with a previous result for plane flow in the presence of gravity.

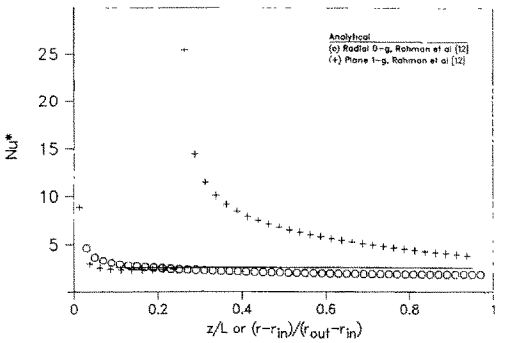

FIG. 8. Heat transfer coefficient for heating with no evaporation adjacent to a constant flux wall.

large Reynolds number, the flow may be supercritical in the entire domain. With a decrease of the Reynolds number, a jump is expected to appear with a subcritical regime. As the Reynolds number is reduced further, the jump may move all the way to the inlet, resulting in completely subcritical flow.

The figure also shows that if the flow enters the control volume with a higher Froude number, it may remain supercritical for a larger distance. The effect of gravity can be also analyzed. For a given flow rate and Froude number, $(z-z^*)$ is inversely proportional to $(g)^{1/3}$. So, for a smaller value of g, the length of the supercritical flow regime is expected to be longer. In the limiting case of zero gravity, a subcritical flow regime is not possible and the flow becomes entirely supercritical.

The predicted film height is compared with the previous numerical solution of Rahman *et al.* [10] for $Re = 89$, $Fr_{in} = 8.6$, $Fr_{out} = 1.0$, $L = 0.14$ m and $\nu = 7.4 \times 10^{-6}$ m^2 s^{-1} in Fig. 7. The height in the supercritical region is slightly over-predicted, whereas in the subcritical region, the height becomes flatter than the numerical solution. In the numerical computation of Rahman *et al.* [10] a critical outflow condition is assumed to be present at the exit, whereas in the analytical solution this condition was not imposed.

4.4. *Radial flow in the presence of gravity*

For radial flow in the presence of gravity, the equations of motion (equations (34)–(36)) can be expressed as

$$\left(\frac{5}{6} - Fr^2\right)\frac{dFr}{dR} = -\frac{5Fr+3Fr^3}{6R} + \frac{15}{4}Fr^{11/3} \quad (49)$$

where

$$R = \frac{r}{(\nu^2/g)^{1/3}\, Re^{5/3}}. \quad (50)$$

Here, we can also notice that a critical condition is arrived at $Fr = 0.913$. This confirms that a critical condition in the flow depends on the velocity profile used for the analysis. The double-valued nature of the solution and the possibility of a hydraulic jump still exists. The solution is presented in Fig. 5 for different values of R^*. Analogous to plane flow, the critical radius R^* corresponds to $Fr = 0.913$. As discussed before, a smaller value of R^* indicates that the flow starts up at a smaller radius where the effects of curvature are important. This fact is quite evident in the figure. The curve for $R^* = 100$ coincides with the plane flow solution. At this situation, the effect of curvature is negligible. Also, at $R^* = 0.5$ and 1, the Froude number attains a minimum in the subcritical regime. This indicates that if a jump happens before that radial location, the film height may still increase in the subcritical region, attain a maximum and then diminish further downstream. This phenomenon is not present in plane flow and at flows with large values of R^*, where the film height decreases monotonically in the subcritical region. It can also be noticed that equation (49) reduces to equation (44) as $R \to \infty$. So, the plane flow may be treated as a limiting case of radial flow where $R \to \infty$.

4.5. *Analysis of heat transfer*

The heat transfer behavior can be solved by integrating equation (37) with the substitution of equation (28) for the temperature profile.

Different thermal boundary conditions are considered in the present study. They are isothermal and uniform flux conditions at the solid wall and evaporation and pure heating without evaporation on the free surface. The heat transfer coefficient for these cases are defined as

$$h = \begin{cases} q_w/(T_w - T_b), & \text{for heating} \\ q_w/(T_w - T_{sat}), & \text{for evaporation.} \end{cases} \quad (51)$$

A general expression for the Nusselt number can be evaluated from equations (30)–(33)

$$Nu^* = \begin{cases} \dfrac{B}{\dfrac{5}{8}B + \dfrac{9}{20}C}, & \text{for heating} \\ \dfrac{B}{B+C}, & \text{for evaporation.} \end{cases} \quad (52)$$

A complete analytical solution is possible for the case of heating, when the free surface is assumed to be adiabatic in nature. For this case, $Nu^* = 2.5$ for both isothermal and uniform flux wall conditions.

Note that Nu^* is a function of the heat transfer coefficient and film height, both of which change with location on the plate. A comparison of this result with the previous numerical solution of ref. [12] is shown in Fig. 8. For radial flow at zero gravity ($Re_{in} = 404$, $Pr = 7$, $r_{in} = 0.05$ m, $r_{out} = 0.2$ m, $\delta_{in} = 0.005$ m, $T_{in} = 20°C$, $q_w = 1000$ W m^{-2}, $\nu = 7.4 \times 10^{-6}$ m^2 s^{-1}, $k = 0.4$ W m^{-1} K^{-1}), the numerical Nusselt number starts at a higher value and then approaches an asymptotic limit as the flow moves downstream. This limiting value is somewhat lower than the analytical prediction. This indicates that the true temperature profile is somewhat flatter than the parabola assumed here. For plane flow in the presence of gravity ($Re = 89$, $Fr_{in} = 8.6$, $Fr_{out} = 1.0$, $Pr = 7$, $L = 0.14$ m, $T_{in} = 20°C$, $q_w = 1000$ W m^{-2}, $\nu = 7.4 \times 10^{-6}$ m^2 s^{-1}, $k = 0.4$ W m^{-1} K^{-1}), the subcritical and supercritical heat transfer coefficients approach the analytically predicted value as the flow moves downstream with the development of the temperature profile.

For an isothermally heated wall with evaporation on the free surface, an expression for the Nusselt number can be derived by integrating equation (37) using equation (28) for the temperature profile and boundary conditions. The result is

$$Nu^* = 1 - \frac{C_0}{\left(\frac{T_{sat}}{T_w} - 1\right)} \exp\left[\beta(z)\right] \qquad (53)$$

where

$$\beta(z) = \frac{80}{7} \frac{\alpha}{Q} \int_0^z \frac{dz}{\delta}. \qquad (54)$$

Here C_0 is the value of C at one location in the flow, where integration should start.

The expressions for Nu^* are true both for the cases where the gravity is finite and infinitesimally small. The actual heat transfer coefficient, however, will be different because of different distributions in the film height.

5. CONCLUSIONS

A systematic analysis of thin film flows in zero gravity and non-zero gravity environments is performed and their implications in a real flow problem under micro-gravity conditions is discussed. The analysis is carried out in two parts. First, the hydrodynamics of the flow is studied for uniform one-dimensional velocity with any given friction factor. Next, the flow field and heat transfer coefficient are determined using the Pohlhausen integral method.

It is found that in the complete absence of gravity, the flow is supercritical, where even for a relatively small, but not negligible gravity, two potential flow regimes—supercritical and subcritical—may be present. The two regimes are separated by a jump where large changes of film height take place. In the presence of friction, both supercritical and subcritical flows move towards a critical condition. The flow regime is characterized by the Froude number, whereas the Reynolds number indicates the relative importance of the inertial and viscous effects.

For plane flow, it is found that in the absence of gravity, the film height increases linearly with distance. When gravity is present, the film height increases monotonically in the supercritical region, encounters a jump and then decreases further downstream in the subcritical region. The heat transfer coefficient in this situation is characterized by $Nu^* = 2.5$, both for isothermal and uniformly heated walls with no evaporation from the free surface.

For radial flow it is found that in addition to the Froude and Reynolds numbers, the inlet radius is an important parameter, which carries the effects of curvature in the flow. At large values of the inlet radius, a plane flow situation is approached. Here, in the presence of gravity, the film height may increase or decrease depending on the flow rate, radial location and Froude number. The comparison of the results with previous numerical solutions shows reasonably good promise that the analytical method presented here can act as a useful tool to easily obtain approximate results for any given flow situation in a normal gravity or microgravity environment.

Acknowledgement—Funding for this work was provided by the NASA Goddard Flight Center, Greenbelt, Maryland, under contract NAG 5-956. The technical assistance provided by Mr Ted Swanson of NASA is appreciated.

REFERENCES

1. V. G. Levich, *Physiochemical Hydrodynamics*. Prentice-Hall, Englewood Cliffs, New Jersey (1962).
2. G. D. Fulford, The flow of liquids in thin films, *Adv. Chem. Engng* **5**, 151–236 (1964).
3. R. A. Seban and A. Faghri, Wave effects in the transport to falling laminar liquid films, *ASME J. Heat Transfer* **100**(1), 143–147 (1978).
4. A. Faghri and P. Payvar, Transport of thin falling liquid films, *Reg. J. Energy Heat Mass Transfer* **1**(2), 153–173 (1979).
5. A. Faghri and R. A. Seban, Heat transfer in wavy liquid film, *Int. J. Heat Mass Transfer* **28**, 506–508 (1981).
6. G. K. Batchelor, *An Introduction to Fluid Dynamics*. Cambridge University Press, Cambridge (1967).
7. E. J. Watson, The radial spread of a liquid jet over a horizontal plate, *J. Fluid Mech.* **20**(3), 481–499 (1964).
8. Z. H. Chaudhury, Heat transfer in a radial liquid jet, *J. Fluid Mech.* **20**(3), 501–511 (1964).
9. T. L. Labus and K. J. DeWitt, Liquid jet impingement normal to a disk in zero gravity, *ASME J. Fluids Engng* **100**, 204–209 (1978).
10. M. M. Rahman, A. Faghri, W. L. Hankey and T. D. Swanson, Computation of the free surface flow of a thin liquid film at zero and normal gravity, *Numer. Heat Transfer* **17A**, 53–71 (1990).

11. M. M. Rahman, A. Faghri and W. L. Hankey, New methodology for the computation of free surface flows using a permeable wall. In *Porous Media, Mixtures and Multiphase Heat Transfer*, ASME HTD-117, pp. 31–38 (1989).
12. M. M. Rahman, A. Faghri, W. L. Hankey and T. D. Swanson, Prediction of heat transfer to a thin liquid film in plane and radial flows, *ASME J. Heat Transfer* **112**(3), 822–825 (1990).
13. W. M. Kays and M. E. Crawford, *Convective Heat and Mass Transfer*, 2nd Edn. McGraw-Hill, New York (1980).
14. S. Thomas, W. Hankey, A. Faghri and T. Swanson, One-dimensional analysis of the hydrodynamic and thermal characteristics of thin film flows including the hydraulic jump and rotation, *ASME J. Heat Transfer* **112**(3), 728–735 (1990).

ANALYSE DE L'ECOULEMENT FLUIDE ET DU TRANSFERT DE CHALEUR DANS UN MINCE FILM LIQUIDE EN PRESENCE ET EN ABSENCE DE GRAVITE

Résumé—Le comportement hydrodynamique et thermique d'un mince film liquide sur une surface horizontale est analysé pour des écoulement qui s'étalent de façon plane ou radiale. On analyse séparément les situations où la force de pesanteur est complètement absente et où elle est significative et on discute leur adaptation au cas d'un environnement de micro-gravité. En présence de pesanteur, outre le nombre de Reynolds, le nombre de Froude du film est un paramètre important qui détermine les régimes supercritique et subcritique et un saut hydraulique associé. Une solution analytique est possible pour quelques situations d'écoulement, tandis que d'autres nécessitent l'intégration numérique des équations différentielles. Les résultats analytiques approchés se comparent bien avec les solutions numériques bidimensionnelles disponibles.

UNTERSUCHUNG VON STRÖMUNG UND WÄRMEÜBERGANG IN EINEM DÜNNEN FLÜSSIGKEITSFILM MIT UND OHNE SCHWERKRAFTEINFLUSS

Zusammenfassung—Das hydrodynamische und thermische Verhalten eines dünnen Flüssigkeitsfilms, der über eine feste waagerechte Oberfläche strömt, wird sowohl für ebene als auch für sich radial ausbreitende Strömung untersucht. Die Bedingungen, unter denen die Schwerkraft ohne jeglichen Einfluß ist, und diejenigen, unter denen diese sich wesentlich auswirkt, werden getrennt untersucht. Die praktische Bedeutung dieser Vorgänge in einer Umgebung unter den Bedingungen der Mikrogravitation wird erläutert. Bei vorhandener Schwerkraft zeigt sich, daß die Froude-Zahl des Films neben der Reynolds-Zahl ein wichtiger Parameter ist, der die Bereiche überkritischer und unterkritischer Strömung und den damit verknüpften Umschlag festlegt. Unter bestimmten Strömungsbedingungen ist eine geschlossene Lösung möglich, wogegen andere Fälle die numerische Integration der gewöhnlichen Differentialgleichungen erfordern. Es zeigt sich, daß die analytischen Näherungslösungen gut mit den verfügbaren zweidimensionalen numerischen Lösungen übereinstimmen.

АНАЛИЗ ТЕЧЕНИЯ ЖИДКОСТИ И ТЕПЛОПЕРЕНОСА В ТОНКОЙ ПЛЕНКЕ ЖИДКОСТИ ПРИ НАЛИЧИИ И ОТСУТСТВИИ СИЛЫ ТЯЖЕСТИ

Аннотация—Проведен гидро- и термодинамический анализ плоского и радиального течения тонкой пленки жидкости на твердой горизонтальной поверхности. Отдельно рассматриваются ситуации, в которых сила тяжести или полностью отсутствует, или существенна, и обсуждается их практическое приложение к случаю присутствия микрогравитации. Найдено, что при наличии силы тяжести число Фруда для пленки, помимо числа Рейнольдса, также является важным параметром, определяющим за- и докритический режимы течения и связанный с ними гидравлический скачок. Для некоторых случаев течения возможно решение в замкнутой форме, для других необходимо численное интегрирование обыкновенных дифференциальных уравнений. Получено хорошее согласие между приближенными аналитическими результатами и имеющимися двумерными численыыми решениями.